Nuclear Instruments and Methods in Physics Research B 372 (2016) 151–155

Contents lists available at ScienceDirect

Nuclear Instruments and Methods in Physics Research B

journal homepage: www.elsevier.com/locate/nimb

Investigation of electrically-active deep levels in single-crystalline diamond by particle-induced charge transient spectroscopy

W. Kada [a,*], Y. Kambayashi [a,b], Y. Ando [a,b], S. Onoda [b], H. Umezawa [c], Y. Mokuno [c], S. Shikata [d], T. Makino [b], M. Koka [b], O. Hanaizumi [a], T. Kamiya [b], T. Ohshima [b]

[a] Faculty of Science and Technology, Gunma University, Kiryu, Gunma 376-8515, Japan
[b] Japan Atomic Energy Agency, Takasaki, Gunma 370-1292, Japan
[c] National Institute of Advanced Industrial Science and Technology (AIST), 1-8-31 Midorigaoka, Ikeda, Osaka 563-8577, Japan
[d] Kwansei Gakuin Univ., 2-1, Gakuen, Mita, Hyogo 669-1337, Japan

ARTICLE INFO

Article history:
Received 15 September 2015
Received in revised form 15 December 2015
Accepted 28 December 2015
Available online 13 January 2016

Keywords:
CVD diamond
Deep-levels
Alpha particle induced charge transient spectroscopy (APQTS)
Heavy ion induced charge transient spectroscopy (HIQTS)

ABSTRACT

To investigate electrically-active deep levels in high-resistivity single-crystalline diamond, particle-induced charge transient spectroscopy (QTS) techniques were performed using 5.5 MeV alpha particles and 9 MeV carbon focused microprobes. For unintentionally-doped (UID) chemical vapor deposition (CVD) diamond, deep levels with activation energies of 0.35 eV and 0.43 eV were detected which correspond to the activation energy of boron acceptors in diamond. The results suggested that alpha particle and heavy ion induced QTS techniques are the promising candidate for in-situ investigation of deep levels in high-resistivity semiconductors.

1. Introduction

Single-crystalline diamond is regarded as an ideal material for a next-generation power devices since it has excellent electrical, mechanical and thermal properties. In addition, diamond attracts great attention for particle detectors owing to its high radiation tolerance [1–3]. For the development of electronic devices based on diamond, it is important to understand electrically active deep level defects in diamond because they affect device characteristics [4–6]. Thus, for the fabrication of electronic devices with designed characteristics, we have to clarify the origin of defects, such as vacancy-type, impurities and their complex, introduced during crystal growth and/or device fabrication process, and find out techniques to control them [7–9]. Although diamond crystal growth techniques have been advanced in recent years, it is still necessary to develop further crystal growth techniques for high quality crystalline diamond for electronic devices with extremely excellent characteristics.

Deep level transient spectroscopy (DLTS) is widely and commonly used to investigate deep levels in semiconductors [10–12]. However, the general DLTS cannot be well applied to characterizing defects in high-resistive wafers which are often used for radiation detectors. To improve the operability in such high-resistive targets, other approach for deep level evaluation was proposed using laser as an external excitation probe (photo induced current transient spectroscopy: PICTS) [13] and ions (scanning ion deep level transient spectroscopy: SIDLTS) [14–16]. Several defect levels in wide bandgap semiconductors *e.g.* hexagonal (4H) silicon carbide (SiC) substrate were measured from transient properties of charge induced by alpha particles, which is called as alpha particle induced charge transient spectroscopy (APQTS) [17]. Furthermore, similar charge transient spectroscopy using heavy ion microbeams as probe (heavy ion induced charge transient spectroscopy, HIQTS) has been developed in a beam line of the 3MV tandem accelerator at JAEA Takasaki [18]. For SIDLTS and QTS, dense charge (electron hole pairs) can be generated in samples by energetic charged particles even if metal electrode covers on the sample surface. Although most generated electrons/holes are immediately swept away from a sample to electrodes, some of them are trapped by deep level centers. Then, those trapped electrons/holes slowly escape to the conduction/valence band by thermal energy, depending on the activation energy of each trapping centers. These release (detrap) of charge from those traps can be observed in time scales

* Corresponding author. Tel.: +81 277 30 1793.
E-mail address: kada.wataru@gunma-u.ac.jp (W. Kada).

http://dx.doi.org/10.1016/j.nimb.2015.12.044
0168-583X/

of several microseconds, which is longer than that for the charge drift inside of the crystal obtained as a standard IBIC technique. Therefore, the activation energy of carrier trapping deep levels can be obtained by measuring cumulative charges slowly collected from a sample. Using QTS, the analysis of radiation detector based on SiC was successfully performed using focused heavy ion microprobe [17,18]. This suggests that QTS can be widely applicable to the observation of deep levels in other wide bandgap semiconductors such as diamond even with high resistivity. It is also expected that impurity atoms distributed in single crystalline diamond might act as electrically-active deep levels [19,20], if impurities have activation energies in ranges above several hundred meV (because such impurities are not activated to be 100% at room temperature). Especially, it is important to clarify impurities unintentionally doped in diamond during crystal growth in order to understand their effects on device characteristics as well as to improve crystal growth condition for high purity crystals. In this study, we investigate electrically-active deep levels in unintentionally doped single-crystalline diamond using APQTS and HIQTS techniques. Comparing with APQTS results obtained from intrinsic CVD diamond, we discuss unintentionally impurities doped in the diamond.

2. Materials and methods

2.1. Sample preparation

A free-standing single crystal unintentionally doped (UID) (001) diamond substrate with dimension of 3 mm × 3 mm and thickness of 100 μm was fabricated by lift-off process using ion implantation [21]. A seed substrate with the size of 9 × 9 mm^2 was implanted with 2 MeV carbon ions to the dose of 2 × 10^{16} ions/cm^2. After the ion implantation, single crystal diamond was grown on the substrate to the thickness of 100 μm by microwave plasma chemical vapor deposition (CVD) as described in Ref. [22]. The CVD grown layer was lifted-off by etching the graphitized ion implanted layer and the obtained plate was cut into 3 × 3 mm for the fabrication of an ionized particle detector with Ti/Pt/Au electrodes. In addition, a spectroscopic grade of single-crystalline intrinsic CVD diamond wafer with size of 4.6 mm × 4.6 mm with a thickness of 50 μm grown by Diamond Detectors, Ltd was also employed for comparison [23]. Quite low leakage current was observed to be less than 10^{-11} A through metalized uniform Ti/Pt/Au electrodes deposited on both sides of the diamond.

2.2. Experimental setup

Schematic illustration of charge transient spectroscopy (QTS) measurement system used in this study is shown in Fig. 1. APQTS was utilized with an ^{241}Am radiation checking source [17]. The source emits 5.5 MeV alpha particles with radiation activity of approximately 10^6 Bq. The distance of the source to the diamond was adjusted to obtain the average count rate of approximately 10 cps during the measurement. A similar QTS system developed on a heavy ion microbeam line of the 3 MV tandem accelerator at JAEA Takasaki was also used [18]. An ion beam induced charge (IBIC) collection system is also installed in the heavy ion microbeam lines [24–26]. Carbon ions with 9 MeV which is one of the standard beams of the microbeam line was employed as the probe of HIQTS measurement in this study. To avoid damaging to the diamond wafers with heavy ions during HIQTS measurements, microbeam were scanned over detectors with a comparably large area of 400 × 400 μm. Also, average count rate of approximately 20 cps was used for the measurement to reduce the permanent damage induced in the crystal by heavy ions. The diamond detectors on a chip carrier were placed on a sample holder with cartridge heater and copper cold finger cooled by a liquid nitrogen (Lq. N_2) circulation system. The charges generated in diamond detector by ion incidence were collected using a charge sensitive preamplifier (CSP; ORTEC, 142A) and the output signals were recorded using a digital storage oscilloscope (DSO; Agilent, DSO2024A). Positive or negative bias voltage up to 50 V was applied to the detectors during QTS measurement.

Algorithm of the QTS measurement is illustrated in schematic step by step as shown in Fig. 2. Firstly, ion induced charge in time ranges up to a few hundred microseconds was recorded through the CSP by the DSO at various temperatures. Charge detrapped from deep level centers is observed after charge obtained within a sub-microsecond range. Therefore, comparing with standard ion beam induced charge (IBIC), it is necessary to measure charge transient for longer periods in the case of QTS. In this study, several output charge signals (pulse signals) obtained at each temperatures were averaged and decay of charge due to the CSP itself was de-convoluted from the averaged pulse signals as a background in order to obtain the actual transient signal structures as shown in Fig. 2(a). The decay constant of the CSP was determined by the signals obtained from non-damaged silicon and SiC samples. During measurements, temperature of the sample was monitored by thermocouples and the feedback was provided to the heater controller manipulated by the in-house software based on LabVIEW. APQTS were carried out at temperatures ranging from 160 to 360 K while HIQTS were done at temperatures ranging from 180 to 280 K in this study.

Then, rate window signal extraction method, which is similar to the method used in DLTS measurements [27,28], was employed to obtain the differences in the amount of cumulative charges at each time period. The cumulative charges obtained from each time period (from t_1 to t_2) was analyzed at each temperature to obtain the QTS spectrum as shown in Fig. 2(b). For the analyses, some combinations of time constant of t_1 and t_2 [For example, Index 0: (t_1: 2 μs/t_2: 6 μs), Index 1: (t_1: 6.8 μs/t_2: 20.2 μs), and Index 2: (t_1: 15.2 μs/t_2: 45.6 μs) were used for the schematic] were selected to obtain the differences in cumulative charges at each temperature.

As a result, QTS spectra from each time period of t_1 and t_2 (Index 0,1,2...) were obtained from the structures of transient signals obtained at different temperatures. In this study, t_1/t_2 ratio was set equal to 3, however QTS analysis system is capable to process different ratio of the time span which should be optimized to obtain the peak in spectrum. If there are any peak appeared in spectrum, the position of the peak was then analyzed using different sets of the time period (t_1 and t_2) but the same ratio of t_1/t_2. Finally, the peak shift of each QTS peaks would be analyzed in Arrhenius plot as shown in Fig. 2(c). And the activation energy of the peaks would be delivered from the slope of the Arrhenius plot.

3. Results and discussion

Fig. 3 shows (a) current–voltage (I–V) and (b) capacitance–voltage (C–V) characteristics of UID CVD diamond. From the asymmetric structure of reverse and forward current, the characteristics of Schottky diode formed on a p-type wafer can be confirmed. Also, it should be mentioned that negative self-bias of approximately −6 V was applied to the surface of the wafer as shown in I–V characteristics. The carrier concentration in the UID CVD diamond wafer was estimated to be approximately 10^{16}/cm^3 from the $1/C^2$–V curve. The depletion layer of the UID CVD diamond at biases of 50 V which is a standard bias value used for QTS measurements was estimated to be approximately 50 μm. Ions used in this

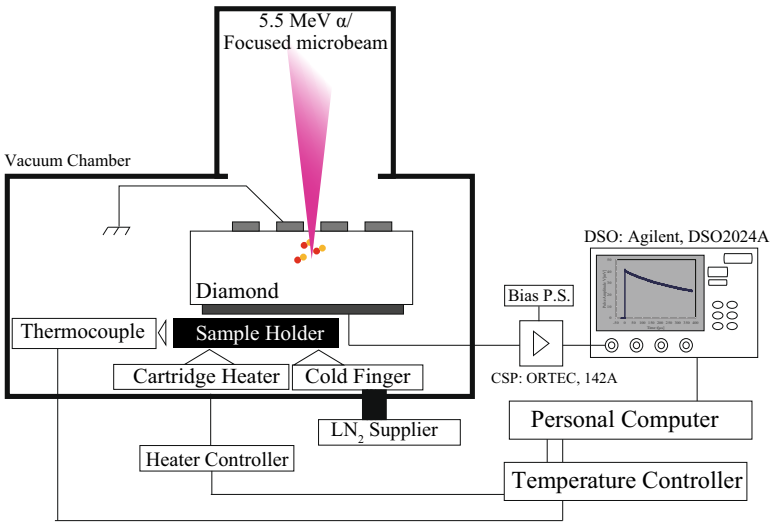

Fig. 1. Schematic illustration of QTS system with an ionized particle probe from a ^{241}Am alpha particle checking source or heavy ion microbeam from a 3 MV tandem accelerator. The charges generated in diamond detector by 5.5 MeV alpha particles or 9 MeV carbon incidence were collected using a charge sensitive preamplifier (CSP; ORTEC, 142A) and the output signals were recorded using a digital storage oscilloscope (DSO; Agilent, DSO2024A).

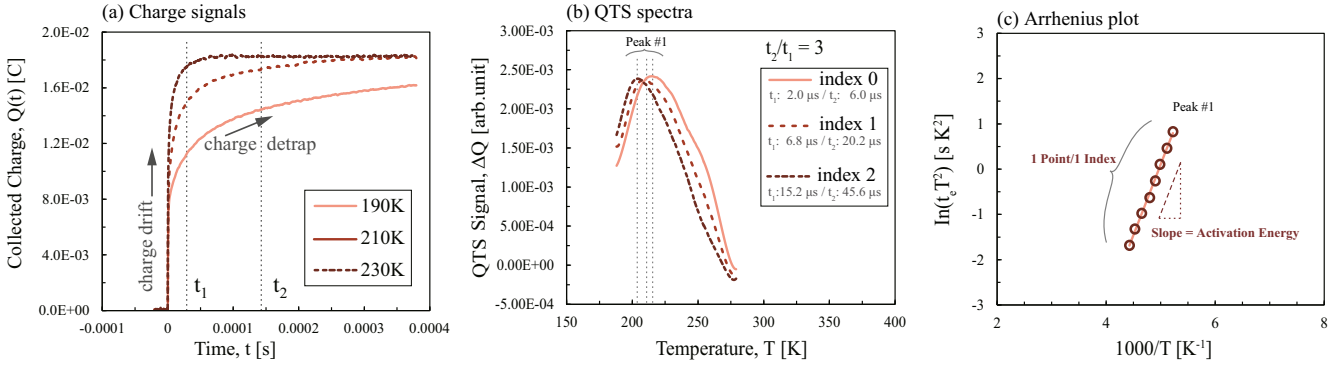

Fig. 2. Scheme of the algorithm of QTS analysis employed in this research. (a) Cumulative charges were obtained from pulse signals at each temperature. (b) QTS spectra of transient pulse signal of 5.5 MeV alpha particles or 9 MeV carbon ions were obtained through the Rate Window Analysis with different set of time period of t_1 and t_2 [For example, Index 0: (t_1: 2 μs/t_2: 6 μs), Index 1: (t_1: 6.8 μs/t_2: 20.2 μs), and Index 2: (t_1: 15.2 μs/t_2: 45.6 μs) were used for the schematic]. (c) Example of an Arrhenius plot of the QTS peak obtained from QTS spectra.

study generate electron–hole pairs in the depletion layer during QTS measurements since the projection ranges of 5.5 MeV alpha particles and 9 MeV carbon ions in diamond are calculated to be 13.64 μm and 4.04 μm, respectively, by SRIM code [29]. Because of small amounts of carrier concentration, the standard DLTS technique could not be performed for the UID crystal and also an intrinsic CVD diamond. Thus, it is concluded that QTS is a useful technique to investigate deep levels in CVD diamond wafer with high-resistivity.

Charge induced by 5.5 MeV alpha particles was measured with different temperatures. Fig. 4 shows the temperature dependence of integrated charge collected for UID CVD diamond with different integration time period (2.0, 6.0, 15.4, and 53.8 μs). The positive bias of 50 V was applied to the diamond during the measurements. The value was normalized with the maximum charge obtained for the temperature range. For the comparison, integrated charge collection from the intrinsic CVD diamond with charge collection time of 15.4 μs was also shown in figure. The charge accumulation was strongly dependent on the integration time period in temperature range between 160 and 240 K. Comparing that of UID and intrinsic diamond, it is expected that this UID CVD diamond supposed to have deep level centers which can release charge in the temperature ranges between 160 and 240 K.

APQTS measurements were carried out for the UID CVD diamond and the intrinsic CVD diamond at a bias voltage of +50 V in temperature ranges from 180 K to 400 K (Fig. 5). The APQTS spectra obtained in the time range from 2 (t_1) to 6 μs (t_2) are plotted in the figure. A single peak (AP1) is obtained at 210 K from the UID CVD diamond while no significant peak is observed from the intrinsic CVD diamond. The obtained result suggests that a deep level center which act as a carrier trap exists in the UID CVD diamond and also, the deep level center might not affect CCE around room temperature because the APQTS spectra for the UID CVD diamond become the background level above 280 K.

For the UID CVD diamond, HIQTS measurements were also carried out. Fig. 6(a) and (b) show HIQTS spectra detected for the UID CVD diamonds with bias voltages of +50 V and −0.2 V, respectively, by 9 MeV-C focused microprobe. It should be mentioned that a reverse bias is applied to the sample even in the case of −0.2 V because of the self-bias on the substrate, and the length depletion layer is estimated to be approximately 20 μm from the *C–V* measurement shown in Fig. 3(b). The HIQTS data were collected in temperature ranges from 180 K to 280 K. A peak (HI1) is observed in HIQTS spectra for the UID CVD diamond biased at 50 V. In the case of applied bias at −0.2 V, the HIQTS spectra are almost the same as those in the case of applied bias at +50 V, and a similar

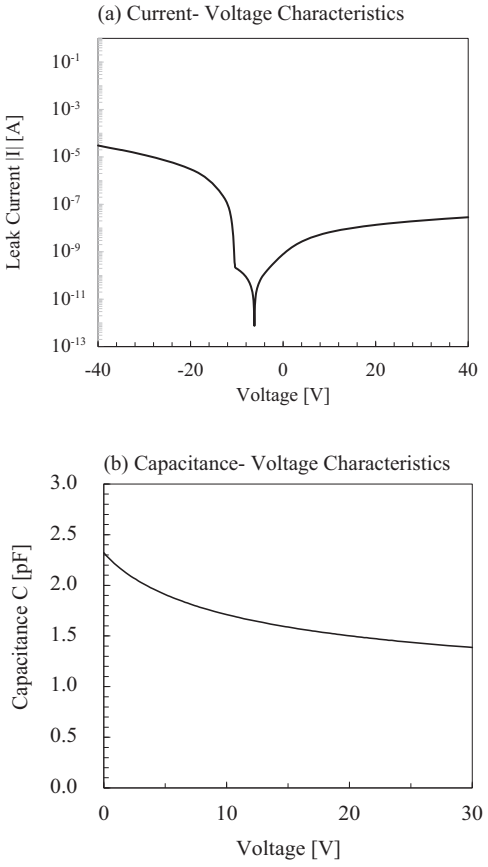

Fig. 3. (a) Reverse and forward current (I)–voltage (V) and (b) capacitance (C)–voltage (V) characteristics of UID CVD diamond based radiation detector. From I–V characteristics, negative self-bias of approximately −6 V was expected to be applied to the surface of the wafer. The carrier concentration of UID CVD diamond was estimated to be approximately 1011 cm^{-2} delivered from C–V characteristics.

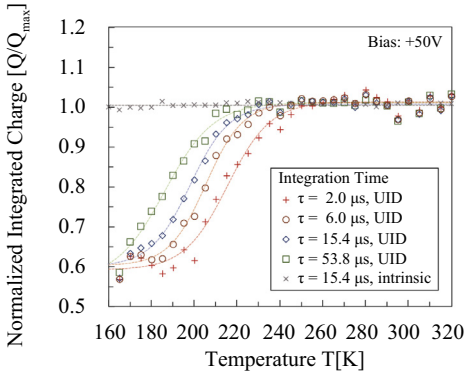

Fig. 4. Temperature dependencies of the integrated charge obtained from UID CVD diamond. The accumulated charge obtained from CSP output was integrated with different time period (2.0, 6.0, 15.4, and 53.8 μs). For the comparison, the integrated charge from intrinsic diamond was also shown in the figure with integration time of 15.4 μs. The amount of the integrated charge was normalized its maximum value. The total amount of the charge accumulation was strongly dependent on the time constant for the charge integration especially in temperature ranges between 160 and 240 K.

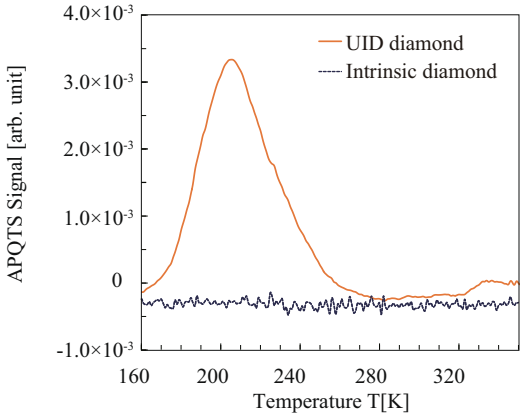

Fig. 5. Example of APQTS spectra of UID CVD diamond and intrinsic CVD diamond detector induced by 5.5 MeV alpha particles. Differences in accumulate charges obtained in the time range from 2 μs (t_1) to 6 μs (t_2) are shown in APQTS spectra of UID and intrinsic CVD diamond. Peak AP1 was appeared in APQTS spectrum obtained from UID CVD diamond and none appeared in that of intrinsic CVD diamond.

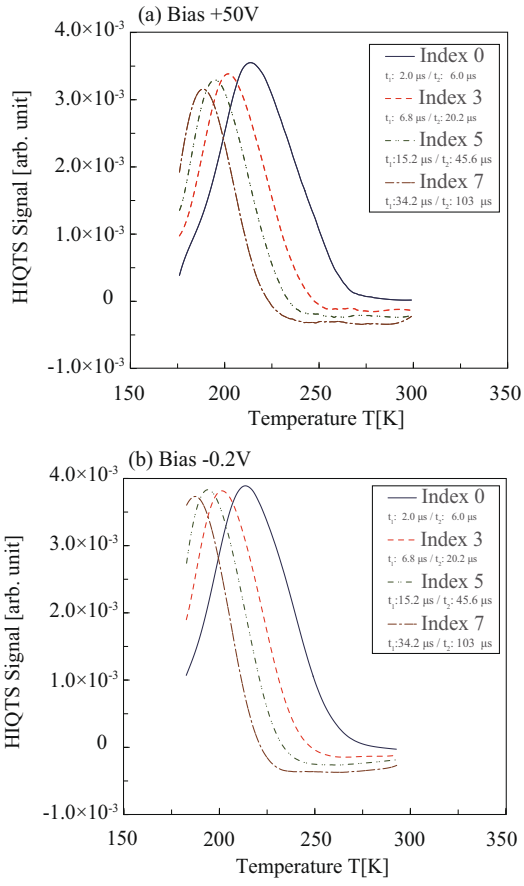

Fig. 6. Example of HIQTS spectra of the UID CVD diamond detector induced by 9 MeV carbon microprobe. Applied voltage of (a) +50 V and (b) −0.2 V were applied to UID diamond. The HIQTS data were collected in temperature ranges from 180 K to 280 K with different time range of (t_1: 2 μs/t_2: 6 μs), (t_1: 6.8 μs/t_2: 20.2 μs), (t_1: 15.2 μs/t_2: 45.6 μs), and (t_1: 34.2 μs/t_2: 103 μs). Peak assigned as HI1 and HI2 were appeared in HIQTS spectra.

peak (HI2) is observed for each spectrum. This result suggests that the observed deep level center is uniformly distributed in the UID CVD diamond.

Fig. 7 shows the Arrhenius plot of AP1, HI1 and HI2 for UID CVD diamond, as shown in Figs. 5 and 6. The activation energy for AP1 is estimated to be 0.43 eV with variation of ±0.04 eV. For HI1 and HI2, the activation energies are estimated to be 0.37 ± 0.02 eV and 0.35 ± 0.01 eV, respectively. Since the activation energy for AP1 corresponds to that for HI1 within error, the origin of deep level

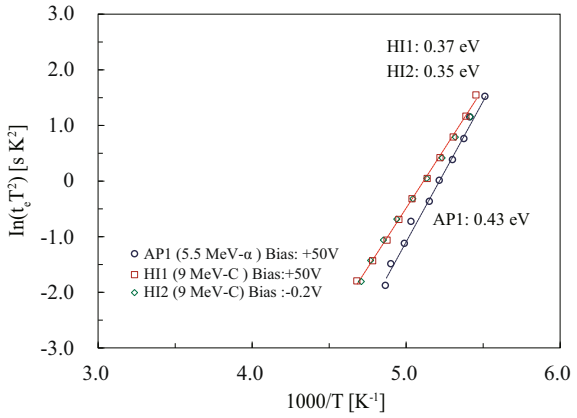

Fig. 7. Arrhenius plots of APQTS (AP1) and HIQTS (HI1 and HI2) peaks obtained from UID CVD diamond. The activation energy for AP1 is estimated to be 0.43 eV with variation of ±0.04 eV. For HI1 and HI2, the activation energies are estimated to be 0.37 ± 0.02 eV and 0.35 ± 0.01 eV, respectively.

center observed by APQTS might be the same as that observed by HIQTS. In addition, from the comparison between HI1 and HI2, it can be concluded that the origin of those deep level is the same. To obtain the higher reproducibility of the measurement result between APQTS and HIQTS, we intend further improvement of the measurement conditions.

Next, the origin of the deep level observed by QTS is discussed. Since the high values of CCE are observed for the UID CVD diamond, the QTS peaks for the UID CVD diamond might not deep levels which harm charge collection properties. In addition, no significant peak is observed in APQTS spectrum of the intrinsic CVD diamond sample, and only UID CVD diamond with an acceptor concentration abound $10^{16}/cm^3$ has QTS peaks. Thus, the origin of QTS peaks for UID CVD diamond must be impurity. In a previous study, Koizumi et al. reported that the activation energy of 0.43 eV was obtained for a donor level in phosphorus doped {1 1 1} CVD diamonds from Hall measurements [30]. However, since phosphorus acts as donor, phosphorus might not be a suitable impurity in the UID CVD diamond. On the other hand, the activation energy for acceptor boron was observed to be 0.34–0.37 eV [31–34]. In addition, it was also reported that the activation energy of conductivity of boron-doped diamond depended on boron/carbon ratio during CVD growth, and estimated to be between 0.11 and 0.43 eV. However, considering temperature dependence of carrier mobility, the activation energy of B acceptor was determined to be approximately 0.35 eV [35]. Therefore, we assume that the peaks obtained for the UID CVD diamond from APQTS and HIQTS measurements is the activation of boron acceptors which are unintentionally doped in UID CVD diamond.

4. Conclusion

Particle-induced charge transient spectroscopy techniques of 5.5 MeV alpha particles (APQTS) and 9 MeV carbon focused microprobes (HIQTS) were applied for the investigation of electrically-active deep levels in high-resistivity unintentionally doped (UID) chemical vapor deposition (CVD) diamond. Deep levels with an activation energy of 0.35/0.37 eV and 0.43 eV were observed in HIQTS and APQTS spectra which seems to be correspond to the activation energy of boron acceptors. Since standard DLTS is not applicable to the measurement of high resistivity UID CVD diamond, the results suggest that alpha particle and heavy ion induced QTS techniques are both promising candidate for in-situ investigation of deep levels in high-resistivity semiconductors.

Acknowledgements

This study was carried out in the framework of the IAEA CRP F11016 "Utilization of ion accelerators for studying and modelling of radiation-induced defects in semiconductors and insulators". This research was partially supported by a MEXT/JSPS Grant-in-Aid for Scientific Research (A) 26249149.

References

[1] J. Isberg, J. Hammersberg, E. Johansson, T. Wikström, D.J. Twitchen, A.J. Whitehead, S.E. Coe, G.A. Scarsbrook, Science 297 (2002) 1670–1672.
[2] H. Pernegger, H. Frais-Kölbl, E. Griesmayer, H. Kagan, Nucl. Instr. Meth. A 535 (2004) 108–114.
[3] F.R.S. Sussmann, CVD Diamond for Electronic Devices and Sensors, John Wiley & Sons Ltd Press, 2009.
[4] P. Bergonzo, A. Brambilla, D. Tromson, C. Mer, B. Guizard, F. Foulon, V. Amosov, Diam. Relat. Mater. 10 (2001) 631–638.
[5] P.J. Sellin, J. Vaitkus, Nucl. Instr. Meth. A 557 (2006) 479–489.
[6] V. Grilj, N. Skukan, M. Jakšić, W. Kada, T. Kamiya, Nucl. Instr. Meth. B 306 (2013) 191–194.
[7] E.-K. Souw, R.J. Meilunas, Nucl. Instr. Meth. A 400 (1997) 69–86.
[8] H. Umezawa, N. Tokuda, M. Ogura, S.-G. Ri, S. Shikata, Diam. Relat. Mater. 15 (2006) 1949–1953.
[9] M. Vila, A.B. Lopes, F.A. Almeida, A.J.S. Fernandes, R.F. Silva, Diam. Relat. Mater. 17 (2008) 190–193.
[10] M. Gong, S. Fung, C.D. Beling, Z. You, J. Appl. Phys. 85 (1999) 7604–7608.
[11] F.C. Beyer, C.G. Hemmingsson, H. Pedersen, A. Henry, J. Isoya, N. Morishita, T. Ohshima, E. Janzen, Phys. Status Solidi RRL 4 (2010) 227–229.
[12] S. Sasaki, K. Kawahara, G. Feng, G. Alfieri, T. Kimoto, J. Appl. Phys. 109 (2011) 13705–13711.
[13] Ch. Hurtes, M. Boulou, A. Mitonneau, D. Bois, Appl. Phys. Lett. 32 (1978) 821–823.
[14] J.S. Laird, R.A. Bardos, C. Jagadish, D.N. Jamieson, G.J.F. Legge, Nucl. Instr. Meth. B 158 (1999) 464–469.
[15] J.S. Laird, C. Jagadish, D.N. Jamieson, G.J.F. Legge, J. Phys. D Appl. Phys. 39 (2006) 1342–1351.
[16] J.S. Laird, C. Jagadish, D.N. Jamieson, G.J.F. Legge, J. Phys. D Appl. Phys. 39 (2006) 1352–1362.
[17] N. Iwamoto, A. Koizumi, S. Onoda, T. Makino, T. Ohshima, K. Kojima, S. Koike, K. Uchida, S. Nozaki, I.E.E.E. Trans, Nucl. Sci. 58 (2011) 3328–3332.
[18] W. Kada, Y. Kambayashi, N. Iwamoto, S. Onoda, T. Makino, M. Koka, T. Kamiya, N. Hoshino, H. Tsuchida, K. Kojima, O. Hanaizumi, T. Ohshima, Nucl. Instr. Meth. B 348 (2015) 240–245.
[19] H.A. Wynands, D.M. Malta, B.A. Fox, J.A. von Windheim, J.P. Fleurial, D. Irvine, J. Vandersande, Phys. Rev. B 49 (1994) 5745–5748.
[20] A.T. Collins, Diam. Relat. Mater. 8 (1999) 1455–1462.
[21] Y. Mokuno, A. Chayahara, H. Yamada, Diam. Relat. Mater. 17 (2008) 415–418.
[22] Y. Mokuno, A. Chayahara, H. Yamada, N. Tsubouchi, Diam. Relat. Mater. 18 (2009) 1258–1261.
[23] S. Gkoumas, A. Lohstroh, P.J. Sellin, Diam. Relat. Mater. 18 (2009) 1338–1342.
[24] J.S. Laird, T. Hirao, H. Mori, S. Onoda, T. Kamiya, H. Itoh, Nucl. Instr. Meth. B 181 (2001) 87–94.
[25] T. Kamiya, T. Hirao, Y. Kobayashi, Nucl. Instr. Meth. B 219–220 (2004) 1010–1014.
[26] W. Kada, T. Kamiya, N. Iwamoto, S. Onoda, V. Grilj, N. Skukan, T. Makino, M. Koka, T. Satoh, M. Jakšić, T. Ohshima, Trans. Mater. Res. Soc. Japan 38 (2013) 279–282.
[27] D.V. Lang, J. Appl. Phys. 45 (1974) 3023–3032.
[28] D.V. Lang, L.C. Kimerling, S.Y. Leung, J. Appl. Phys. 47 (1976) 3587–3591.
[29] J.F. Ziegler, M.D. Ziegler, J.P. Biersack, Nucl. Instr. Meth. B 268 (2010) 1818–1823.
[30] S. Koizumi, H. Ozaki, M. Kamo, Y. Sato, T. Inuzuka, Appl. Phys. Lett. 71 (1997) 1065–1067.
[31] A.T. Collins, E.C. Lightowlers, Phys. Rev. 171 (1968) 843–855.
[32] G.S. Gildenblat, P.E. Schmidt, Handbook Series on Semiconductor Parameters, World Scientific, London, 1996. 58–76.
[33] A. Hatta, S. Sonoda, T. Ito, Diam. Relat. Mater. 8 (1999) 1470–1475.
[34] V.I. Polyakov, A.I. Rukovishnikov, N.M. Rossukanyi, V.G. Ralchenko, Diam. Relat. Mater. 10 (2001) 593–600.
[35] N. Fujimori, H. Nakahata, T. Imai, Jpn. J. Appl. Phys. 29 (1990) 824–827.